CROATICA CHEMICA ACTA CCACAA 53 (3) 485—501 (1980)

CCA-1230

YU ISSN 0011-1643
UDC 541.135
Original Scientific Paper

Application of ASV for Trace Metal Speciation III. Simulated and Experimental Neopolarograms Using Rotated Disk Electrodes

M. Lovrić and M. Branica*

Center for Marine Research, »Ruđer Bošković« Institute Zagreb, Croatia, Yugoslavia

Received February 4, 1980

The digital simulation procedure for neopolarograms using rotated disk electrode is described and the properties of reversible and nonreversible neopolarograms are discussed. The results are compared with experimental neopolarograms of lead in perchlorate medium. The theory of neopolarography using thin mercury film electrodes is developed.

In the first paper of this series[1], the basic principles of neopolarography using HMDE and their applications to trace metal ion speciation were described. In the second one[2], the digital simulation of neopolarograms using HMDE was reported.

Neopolarography is an electrochemical method which consists of several successive ASV cycles at various potentials of pre-electrolysis. The anodic stripping peak current vs. the accumulation potential curves, the so-called neopolarograms or reconstructed d. c. polarograms, shift to a negative direction if the concentration of some ligands in the solution, forming labile complexes with the metal ions investigated, is increased[3]. This shift is parallel to the shift of the d. c. polarogram and therefore is used for the determination of the complexation constants of several metal ions at very low concentration levels[1,3].

The sensitivity of neopolarography can be greatly improved if instead of an HMDE, a rotating, glassy carbon disk, thin mercury film covered in situ electrode (RGCDTMFE) is used[4]. The sensitivity of the HMDE is 10^{-7} (dm^{-3}) of the metal ion[1], while the RGCDTMF can work even at 10^{-9} (dm^{-3}) of the metal ion[5].

The objective of this paper is to investigate the properties of neopolarograms using the RGCDTMFE. For the experimental testing a 2.10^{-8} molar Pb^{2+} in perchloric (pH = 2) medium was chosen. More general research was undertaken using the digital simulation method. For a brief analysis of the results, a mathematical model of neopolarograms under the given conditions was developed.

---

* Taken in part from the M. Sc. thesis of M. L. at the University of Zagreb, 1977.

EXPERIMENTAL

All reagents used were of analytical grade. The following stock solutions were prepared:

0.10151 (mol dm^{-3})	$Pb(NO_3)_2$	(Carlo Erba)
5.06 (mol dm^{-3})	$NaClO_4$	(Kemika)
3.11 (mol dm^{-3})	$HClO_4$	(Kemika)

The $NaClO_4$ and $HClO_4$ solutions were purified by preelectrolysis for 24 hours at —1.3 (V) vs. SCE. All other solutions were prepared by diluting stock solutions. Water used for all solutions was distillated four times, twice using quartz equipment.

A polyethylene voltammetric cell, described by Sipos et al.[6], was used together with a three-electrode system with a rotating disk electrode covered with a thin mercury film which was electrodeposited directly from the investigated experimental solutions to which $2\ 10^{-5}$ (mol dm^{-3}) $HgCl_2$ was added, as described by Florence[4].

The SCE was used as a reference electrode while big glassy carbon rods were used as counter electrodes. The volume of solution was 50 ml. Deaeration was achieved by the application of extra pure nitrogen throughout the entire experiment[7].

For ASV measurements, the »PAR-170 Electrochemistry System« (Princepton Applied Research) with a maximal sensitivity of $4\ 10^{-12}$ A/mm, and linear potential sweep rates from 0.2 mV/s to 500 V/s was used. pH measurements, for a pHM4c (Radiometer) pH meter was used. A potentiostat ASA4c (Tacussel) and a digital voltameter PAR-136 were used for the pre-electrolytical purification of the solutions.

Experimental systems $Pb(NO_3)_2 - NaClO_4 - HClO_4 - HgCl_2$ with the ionic strength of 3.0 and 0.7, pH = 2, lead conc. $2\ 10^{-8}$ (mol dm^{-3}), conc Hg^{2+} 2.10^{-5} (mol dm^{-3}) and conc. $Cl^- = 4\ 10^{-5}$ (mol dm^{-3}) were prepared.

Before the beginning of the experiments, mercury film with a thickness of about 0.05 μm was prepared by electrolysis at —0.8 (V) vs. SCE. The film formed was purified from an amalgam by reoxidation at —0.05 (V) vs. SCE during 2 min. After that, successive ASV cycles between —0.2 (V) and —0.8 (V) vs. SCE with 5 minute depositions at potentials between —0.45 (V) and —0.8 (V) vs. SCE were recorded. The speed of the potential change in the cathodic branch of the voltammetric cycle was 500 mV/s, and in the anodic branch it was 50 mV/s.

Owing to a continuous deposition of mercury during all the cycles, the mercury film grew continuously and at the end of the neopolarogram it reached a thickness of about 0.2 μm.

The recording of each neopolarogram was repeated at least five times.

DIGITAL SIMULATION

The principles of the program for the digital simulation of a neopolarogram and its flow chart have been reported in our previous paper[2]. Because of the different hydrodynamic conditions simulated, some differences were introduced in this program, as described below.

Because of a very thin mercury film on the rotating glassy-carbon electrode, diffusion of the amalgam through the mercury film was ignored, so that the concentration of the amalgam was defined in the following way:

$$c_R = \sum_{j=1}^{T/\Delta t} \left(\frac{i}{nFA}\right)_j \frac{\Delta t}{l} = \sum_{j=1}^{T/\Delta t} \left(\frac{i}{nFA}\right)_j \frac{\Delta t \Delta x}{\Delta x l} = \sum_{j=1}^{T/\Delta t} \frac{FF_j}{HLL}$$

The rotation of the electrode was not simulated, but the existence of the constant diffusion layer δ in the neighborhood of the rotating electrode surface (defined by the Levich expression[8] $\delta = 1.60812\ D_{ox}^{1/3}\ \nu^{1/6}\ \omega^{-1/2}$) was expressed by a finite number of space increments in the solutions, through which a diffusion layer could grow. The number of increments corresponding to the δ thickness was NDL = $= \delta/\Delta x$. The increment NDL + 1 had a concentration of c_{ox}^* as the whole bulk of the solution. In such a way, axial and radial movement of the solution in the diffusion layer was neglected, but we thought this approximation to be sufficiently precise for our purposes.

The basic neopolarogram was simulated under the conditions for thin mercury film rotating disk electrodes. The mercury film thickness was $1 = 0.5\ 10^{-6}$ (m), the rotation speed of the electrode was $\omega = 25$ (s^{-1}), the duration of accumulation was

$T = 300$ (s), the anodic stripping speed was 0.1 (V s^{-1}), both diffusion coefficients values were 4 10^{-6} (cm^2 s^{-1}), the standard potential was fixed at zero $E_0 = 0.000$ (V), the number of the electrons involved was n = 1, the transfer coefficient was $\alpha = 0.5$ and the standard constant of the electrochemical reaction rate was $k_s = 40$ (cm s^{-1}) in order to provide a high reversibility of reaction. During accumulation and anodic stripping oxidation, an increase of mercury at the electrode was neglected and electrode rotation was kept unchanged. The program constants were: $E = 0.00002$ (V); $DD = 0.3$; $\Delta t = 2\ 10^{-4}$ (s); $\Delta x = 5.15\ 10^{-5}$ (cm) in the voltammetrical phase, and $\Delta t = 2\ 10^{-2}$ (s); $\Delta x = 5.15\ 10^{-4}$ (cm) in the accumulation phase.

Because of this change in increment values, subroutine CORR which redefined the concentrations of depolarizer in the diffuse layer after the end of the accumulation period were introduced and the values of all the expressions normalized by the Δx, Δt or $\Delta x/\Delta t$ ratio (*FF*, *HLL*, *NDL*, k_s, etc.) were changed.

Instead of anodic or cathodic current, an adimensional function of the current

$$APPN = \frac{i}{n\,F\,A\,C_{ox}^{*}\,D_{ox}^{1/2}\,(F\,\Delta E/RT\,\Delta t)^{1/2}}$$

was taken as the result of simulation.

The program was written in FORTRAN and run on a UNIVAC 1110 (Sperry rand) computer. Logarithmic analyses of polarograms were calculated on a PDP 11 DIGITAL computer.

Mathematical Model of a Neopolarogram

To interpret the digital simulation results better, a small mathematical model of a neopolarogram built on the same principles as the digital simulation model was developed. This means that axial and radial movements of the solution were neglected and that only the existence of the constant diffusion layer at the surface of the rotating disk electrode was taken into account. Such an approach led us to divide the whole process into two phases. In the first phase, the thickness of the diffusion layer in the solution is smaller than the thickness of the constant diffusion layer defined by the Levich expression[8]. The depolarizer concentration on the surface of the electrode during this phase can be defined by the expression for stationary plane semi-infinitive diffusion:

$$c_{ox}(0) = c_{ox}^{*}\,(1 - I_{ox}^{\circ}) \tag{1}$$

where $I_{ox}^{\circ} = \int_0^t \frac{\Phi(\tau)\,d\tau}{(\pi\,(t-\tau))^{1/2}}$ surface conc. integral

$$\Phi = \frac{i}{nFD_{ox}^{1/2}\,c_{ox}^{*}}$$ normalized current

c_{ox}^{*} = the bulk conc. of depolarizer

In the second phase, the thickness of the diffusion layer in the solution is constant and defined by the Levich expression, but the concentration gradient of the depolarizer depends on its surface concentration and varies with time.

$$\left(\frac{dc_{ox}}{dx}\right)_{0<x<\delta} = \frac{c_{ox}^{*} - c_{ox}^{(0)}}{\delta}$$

$$\left(\frac{dc_{ox}}{dx}\right)_{x=0} = \frac{i}{nFAD_{ox}}$$

so

$$C_{ox}(0) = c_{ox}^{*}\,(1 - \delta\,D_{ox}^{-1/2}\,\Phi) \tag{2}$$

where,

δ — the thickness of the diffusion layer

D_{ox} — the diffusion coefficient

Φ — the normalized current

The diffusion of the amalgam through the mercury film on the electrode was also neglected, so that the concentration of the amalgam on the electrode surface was defined by:

$$C_R(0) = D_{ox}^{1/2} c_{ox}^* l^{-1} \int_0^t \Phi \, dt \tag{3}$$

where, l is the thickness of the mercury film at the electrode.

At the end of the first phase, the concentration of the amalgam may be calculated by introducing the eqs. (1) and (3) in the eq. (4) for the depolarization current:

$$\Phi = k_s D_{ox}^{-1/2} e^{-\alpha\varphi} c_{ox}^{*-1} (c_{ox}(0) - c_R(0) \, e^{\varphi}) \tag{4}$$

This gave us:

$$\Phi = L_1 - L_1 I_{ox}^{\circ} - L_1 \Lambda_1 \int_0^t \Phi \, d\tau \tag{5}$$

where

$$\varphi = \frac{nF}{RT}(E - E^{\circ})$$

k_s = the standard constant of the electrode reaction rate

α — the transition coefficient

$L_1 = k_s D_{ox}^{-1/2} e^{-\alpha\varphi}$

$\Lambda_1 = D_{ox}^{1/2} l^{-1} e^{\varphi}$

The solution of the eq. (5) and its introduction into the eq. (3) gave the expression for the concentration of the amalgam at the end of the first phase ($t = t_1$):

$$B = c_R(0) = c_{ox}^* e^{-\varphi} - D_{ox}^{1/2} c_{ox}^* l^{-1} L_1 (L_1^2 - 4L_1\Lambda_1) \cdot (y_1^{-1} e^{y_1^2 t_1} \operatorname{erfc}(y_1 t_1^{1/2}) - y_2^{-1} e^{y_2^2 t_1} \operatorname{erfc}(y_2 t_1^{1/2})) \tag{6}$$

where

$$y_{1,2} = -\frac{1}{2}(L_1 \pm (L_1^2 - 4L_1\Lambda_1)^{1/2})$$

B — the abbreviation of the eq. (6)

For reversible processes, the eq. (6) becomes

$$B_R = c_R(0) = c_{ox}^* e^{-\varphi} \; (1 - e^{\Lambda_1^2 t_1} \operatorname{erfc}(\Lambda_1 t_1^{1/2})) \tag{6a}$$

In the second phase, the time is measured again from zero, so in the eq. (3) the expression B has to be added. If, now, eqs. (2) and (3) are introduced into the eq. (4), we obtain the expression for the depolarization current during the accumulation period and the integral of the depolarization current over the total time of the accumulation (T) which is directly proportional to the concentration of the accumulated amalgam.

eqs. 2), 3), 4)

$$L\Phi = M - N \int_0^t \Phi \, d\tau \tag{7}$$

where,

$$L = 1 + k_s \delta D_{ox}^{-1/2} e^{-\alpha\varphi}$$

$$M = k_s D_{ox}^{-1/2} (1 - B c_{ox}^{*-1} e^{\varphi}) e^{-\alpha\varphi}$$

$$N = k_s l^{-1} e^{(1-\alpha)\varphi}$$

B = defined by the eq. (6)

The Laplace transformation gives

$$\Phi = \frac{M}{L} \exp\left(-\frac{N}{L} t\right) \tag{8}$$

$$I = \int_0^T \Phi \, dt = \frac{M}{N} \left(1 - \exp\left(-\frac{N}{L} T\right)\right) \tag{9}$$

Voltammetric calculations were not made because, according to data in the literature[9], the peak current is a linear function of the integral of the electrolysis current over the accumulation time. Therefore, it was concluded that the analysis of this integral would be the most important step in all the neopolarogram analyses.

RESULTS

The Experiments with Lead in Perchlorate Medium

The controlling d. c. polarographic measurements of lead in the system $Pb(N_3)$—$NaClO_4$—$HClO_4$ (the ionic strength of 0.7), pH range from 0.73 to 2.3, gave the half-wave potential value of —0.387 (V) vs. the SCE.

Voltammetric measurements in the medium $NaClO_4$—$HClO_4$—$HgCl_2$ (the ionic strength of 0.7 and 3.0) gave results which are in a good agreement with the literature. The intensity of peak current is a linear function of the concentration of the depolarizer and the time of accumulation. The peak potential is negatively shifted from the standard electrochemical potential of lead. Owing to an increase in the mercury layer on the electrode during the experiment, the peak potentials shift continuously to more positive values. In the solutions with an ionic strength of 0.7, peak potentials are in the range between —0.465 (V) and —0.440 (V) vs. the SCE, while in the solutions with an ionic strength of 3.0 they are between —0.440 (V) and —0.420 (V) vs. the SCE.

Following the dependence of anodic current peak intensity over the accumulation potential, we have constructed neopolarograms and their logarithmic analyses. Figure 1. shows a typical neopolarogram and its logarithmic analysis, which is a straight line with a slope value of about 2. The point corresponding to the half-wave potential was chosen as a keypoint of the neopolarogram, as done by Zirino and Kounaves[10] and was given the name of quasihalf-wave potential ($E_{1/2}$*). No stochastic connection exists between $E_{1/2}$* and the conc. of Pb^{2+}.

Table I and Table II shows the composition of experimental solutions and the key-point values of the neopolarogram. Some discrepancies in $E_{1/2}$* values are observed. According to the theory of Zirino and Kounaves[10], these can be compared with the discrepancies in the values of mercury layer thickness at the electrode found in different experiments. During accumulation,

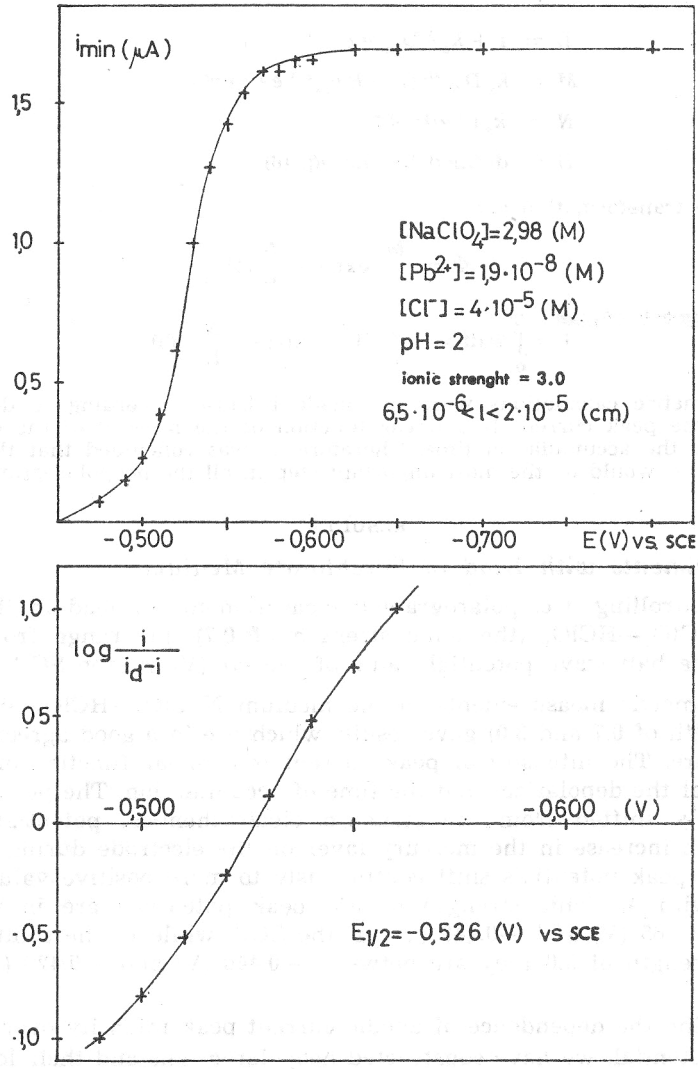

Figure 1. Neopolarogram of lead in a perchloric medium and its log. analysis.

values of mercury layer thickness were counted from the integral of the cathodic current. However, this procedure is not very certain because of some possible effects induced by an oxygen and hydrogen reduction. Therefore, the results obtained are rather imprecise.

Figure 2. shows the statistical distribution of $E_{1/2}$* values in solutions with the ionic strength of 0.7 and 3.0. A slight shift of the most probable values in a positive direction with an increase in the i. s. value may be observed. The average value of $E_{1/2}$* in the solutions with the i. s. of 0.7 is —0.538 (V) and in the solutions with the i. s. of 3.0 it is —0.527 (V). This diffe-

TABLE I

Results of Neopolarographic Measurements of Lead in $NaClO_4 - HClO_4$ Medium (i. s. = 0.7 : pH = 2 : $Pb^{2+} = 2\ 10^{-8}$ mol dm^{-3})

$[HClO_4]$	$[NaClO_4]$	$[Pb(NO_3)_2]$	pH	E_p(V)	$I_{max}(\mu A)$	$E^*_{1/2}$(V)
0,700	-	$2\cdot10^{-8}$	0,16	-0,455	1,80	-0,553
0,500	0,200	$2\cdot10^{-8}$	0,30	-0,453	2,45	-0,536
0,200	0,500	$2\cdot10^{-8}$	0,73	-0,453	2,45	-0,544
0,100	0,600	$2\cdot10^{-8}$	1,05	-0,450	2,80	-0,526
0,050	0,650	$2\cdot10^{-8}$	1,31	-0,447	2,80	-0,532
0,020	0,680	$2\cdot10^{-8}$	1,75	-0,440	2,60	-0,534
0,010	0,690	$2\cdot10^{-8}$	2,07	-0,448	2,70	-0,541
0,005	0,695	$2\cdot10^{-8}$	2,32	-0,450	3,50	-0,536

TABLE II

*Results of Neopolarographic Measurements of Lead in $NaClO_4 - HClO_4$ Medium (i. s. = 3.0 : pH = 2: conc. $Pb^{2+} = 3\ 10^{-8}$ mol dm^{-3}: conc. $Cl^- = 4\ 10^{-5}$ mol dm^{-3} except *conc. $Cl^- = 8\ 10^{-5}$ and **conc. $Cl^- = 1\ 10^{-6}$ mol dm^{-3})*

Nr	$[Pb^{2+}]\cdot10^8$(M)	$I_1\cdot10^6$ (m)	$I_2\cdot10^6$(m)	$E_{1/2}$(V)vs SCE	„n"
1	3,2	0,61	9,61	-0,528	1,57
2	3,2	0,0043	0,042	-0,540	2,0
3	4,5	0,29	3,76	-0,537	2,07
4	4,8	3,86	4,5	-0,529	1,81
5	2,6	0,25	3,13	-0,523	2,0
6	1,7	0,03	26,3	-0,524	1,82
7	1,9	0,03	0,45	-0,526	1,81
8	2,1	0,05	1,23	-0,525	1,90
9	1,7	0,52	2,25	-0,519	1,76
10	2,7	0,6	1,93	-0,515	1,80
11*	3,0	0,17	2,59	-0,512	2,9
12**	4,3	4,77	11,27	-0,512	2,12

rence may be ascribed to the following change in the solution parameters: the lead coefficient of diffusion in the solutions with the i. s. of 0.7 has a value of 0.9 10^{-5} ($cm^2\ s^{-1}$) and in the solutions with the i. s. of 3.0 the value is 0.64 10^{-5} ($cm^2\ s^{-1}$); the kinematic viscosity in the solutions with the i. s. of 0.7 has the value of 0.87 10^{-2} ($cm^2\ s^{-1}$) and in the solution with the i. s. of 3.0 the value is 0.85 10^{-2} ($cm^2\ s^{-1}$) (data obtained by our measurements). Most likely, this is the reason for peak potential differences between these solutions. The general shift of the neopolarogram in a negative direction, related to the position of the d. c. polarogram, confirms the theory of Zirino and Kounaves[10] on the influence of the mercury layer thickness upon the quasi half-wave potential of the neopolarogram.

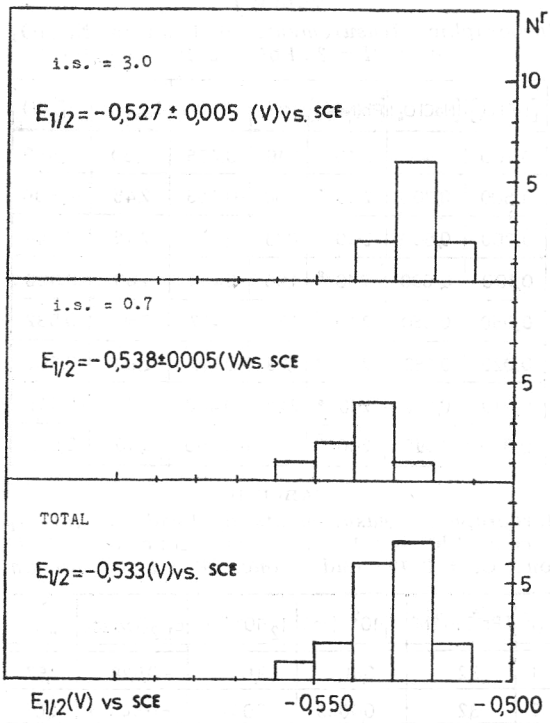

Figure 2. Distribution of the half-wave potentials of neopolarograms of lead in the system $NaClO_4$—$HClO_4$—$HgCl_2$.

Digital Simulation of Neopolarograms

Figure 3. shows a simulated one-electron neopolarogram while Figure 4 shows its logarithmic analysis. The half-wave potential is $E_{1/2}^* = -0.253$ (V) vs. E^0 and the slope of the log. analysis is 58 mV/decade unit. The shape of the log. analysis curve is in good agreement with Shuman and Cromer's experiments with a Tl^+/Tl system.

Dependences of quasi half-wave potential over the values of mercury layer thickness, accumulation time values, electrode rotation speed values and anodic stripping speed values are in good agreement with the theories of Zirino and Kounaves[10] (linear dependence over log (l), log (ω), and log (T) values) and Toni and Roe[9] (independence over the values of the logarithm of the anodic stripping speed).

Figure 5. shows the dependence of the logarithmic analyses of neopolarograms over the standard constant of the electrochemical reaction rate (k_s).

All curves fall down at the bottom in a straight line with a slope of —60 mV/d. a. However, discrepancies appear in the middle range: quasi-reversible processes ($k_s > 4\ 10^{-4}$ cm s^{-1}) show a slope greater than 60 mV/d. u., while irreversible processes ($k_s < 4\ 10^{-4}$ cm s^{-1}) have a slope smaller than 60 mV/d. u. for the same range. Half-wave potentials of neopolarograms shift in a negative direction depending on the value for k_s, and specifically after $k_2 = 1\ 10^{-3}$ cm s^{-1}, as shown in Figure 6.

The simulation of a two-electron neopolarogram (all parameters, except for the number of electrons transferred, are the same as for a one-electron neopolarogram) gives a greater slope of log. analysis (27 mV/d, u.) and a shift of the half-wave potential in the positive direction ($E_{1/2}^{+} = -0.125$ (V) vs. E_o).

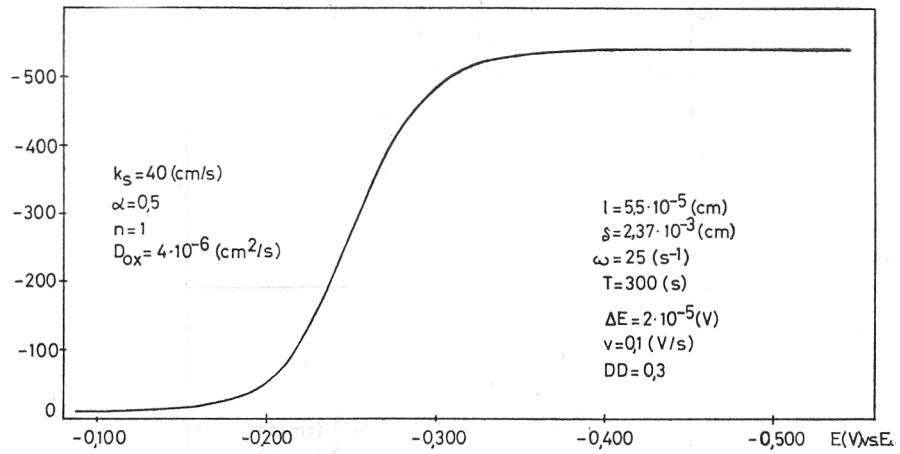

Figure 3. One-electron neopolarogram (simulation).

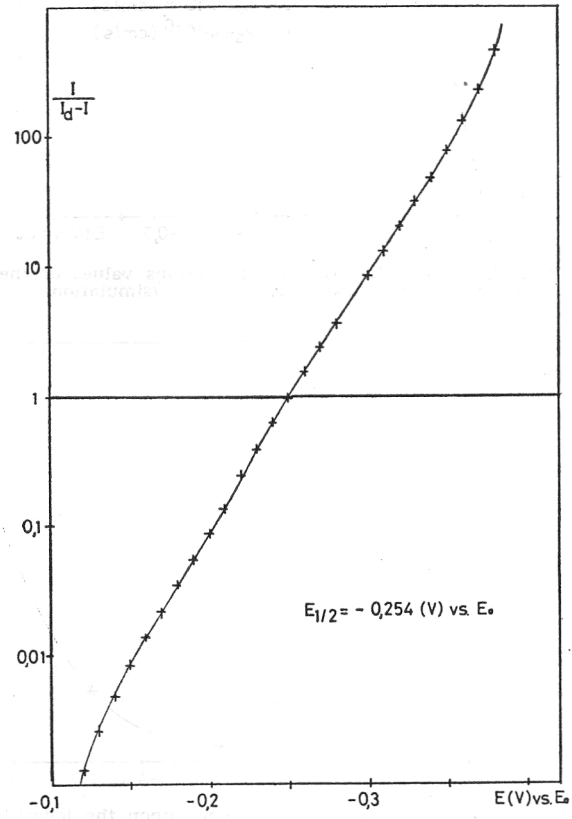

Figure 4. Logarithmic analysis of simulated one-electron neopolarogram from Figure 3.

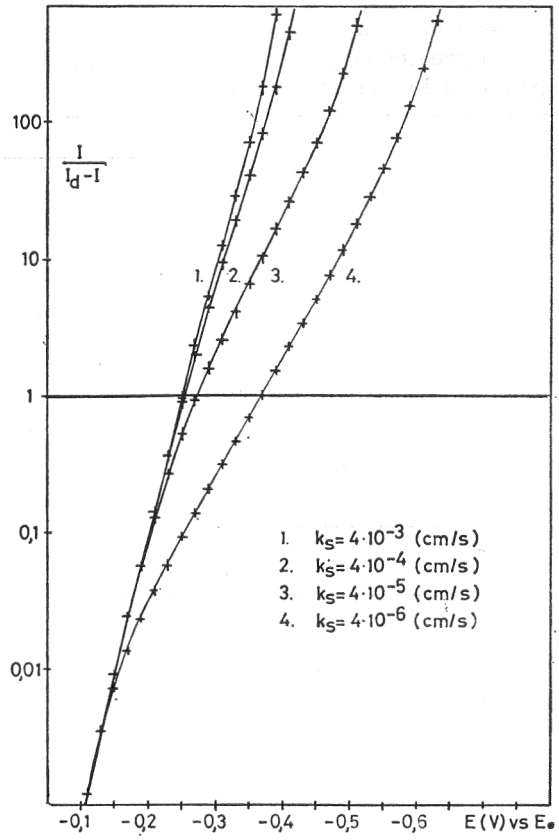

Figure 5. Logarithmic analysis of neopolarograms at various values of the standard constant of the electrochemistry reaction rate (simulation).

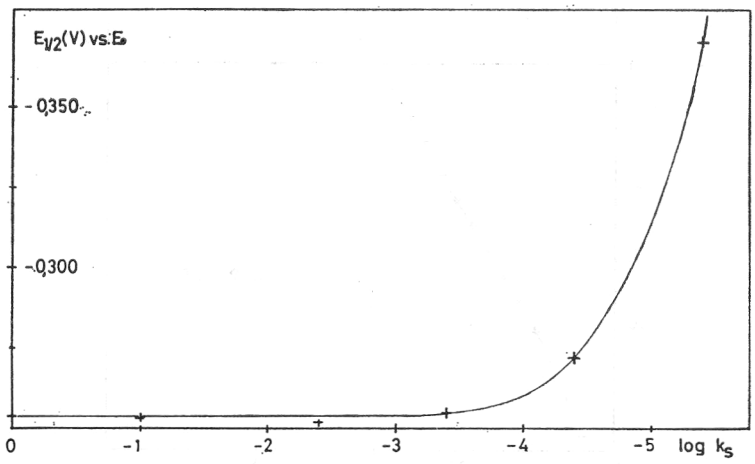

Figure 6. Neopolarogram half-wave potential dependence upon the logarithm of the standard constant of the electrochem. reaction rate (simulation).

The control of the program for digital simulation was achieved by the simulation of a lead neopolarogram under experimental conditions. Figures 7. and 8. illustrate the results obtained by using the electrochemical constants of lead (k_s, α, E_o, D_{ox}, etc.) compiled from the literature and the experimental

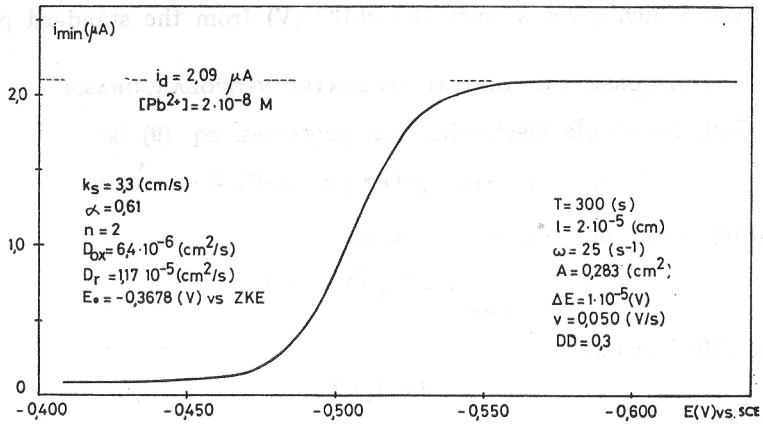

Figure 7. Neopolarogram of lead (simulation).

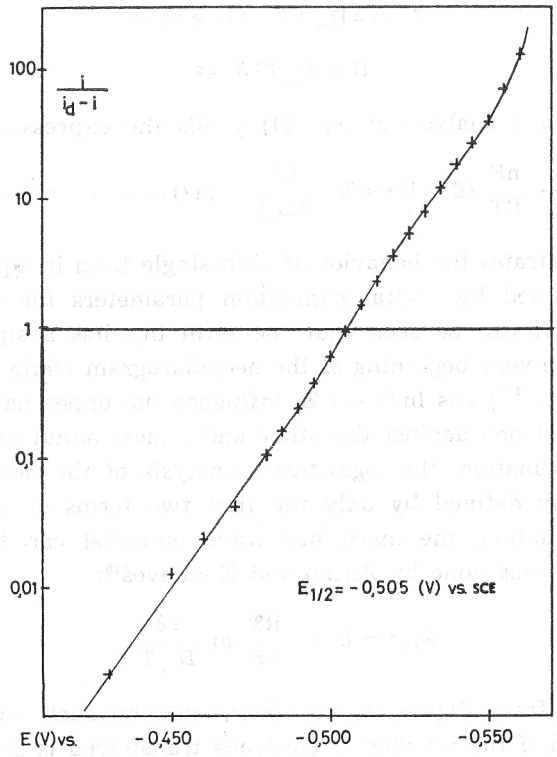

Figure 8. Logarithmic analysis of the neopolarogram of lead (simulation).

constants (l, δ, ω, etc). The limiting current value of the simulated neopolarogram was 2.09 μA, which corresponds to the experimental value for a lead concentration of 2 10^{-8} (mol dm^{-3}). The logarithmic analysis shows the known properties of the two-electronic waves, and the halfwave potential of —0.505 (V) vs. SCE, which gives a shift of —0.137 (V) from the standard potential.

DISCUSSION OF DIGITAL SIMULATED NEOPOLAROGRAMS

For fast, reversible electrochemical processes, eq. (9) is:

$$I = lD_{ox}^{-1/2}\,(1 - B_R\, c_{ox}^{*-1}\, e^{\varphi})\,(1 - e^{-D_{ox}\, Tl^{-1}\, \delta^{-1}\, e})\, e^{-\varphi} \tag{10}$$

The limiting value of I for $E \to -\infty$ is:

$$\lim_{\epsilon \ll \epsilon^0} I = D_{ox}^{1/2}\, T\, \delta^{-1} = I_g$$

Thus, eq. (10) becomes

$$I = I_g\, \varepsilon\, Z \tag{11}$$

where

$$\varepsilon = e^{A_1^2\, t_1}\, \mathrm{erfc}\,(A_1\, t_1^{1/2})$$

$$Z = l\, \delta\, D_{ox}^{-1}\, T^{-1}\, (1 - e^{-UT})\, e^{\varphi}$$

$$U = D_{ox}\, l^{-1}\, \delta^{-1}\, e^{\varphi}$$

The logarithmic analysis of eq. (11) yields the expression:

$$\ln \frac{I}{I_g - I} = -\frac{nF}{RT}\,(E - E^0) + \ln \frac{l\,\delta}{TD_{ox}} + \ln\,(1 - e^{-UT}) + \ln\varepsilon - \ln(1 - \varepsilon\, Z) \tag{12}$$

Table III ilustrates the behavior of each single term in eq. (12) (numerical calculations obtained by digital simulation parameters for a one-electronic neopolarogram). It can be seen that the term $\ln \varepsilon$ has a significant contribution only in the very beginning of the neopolarogram while on the contrary, the terms $\ln (1 - e^{-UT})$ ans $\ln (1 - \varepsilon\, Z)$ influence the upper part of the neopolarograms, but act one against the other and almost annul each other. Thus, to a first approximation, the logarithmic analysis of the neopolarogram can be quite correctly defined by only the first two terms of eq. (12). From a thus reduced equation, the quasi half-wave potential can be expressed in the same way as was done by Zirino and Kounaves[10]:

$$E_{1/2}^{*} = E^0 + \frac{RT}{nF} \ln \frac{l\,\delta}{D_{ox}\, T}$$

As can be seen from Figure 9., mistakes made by such an approximation may be neglected if the number of electrons transferred is 2 or more (numerical calculations from eq. (12) on the basis of digital simulation parameters).

TABLE III

Comparison of the Behavior of the Different Terms from the Equation (12) (Reversible Neopolarogram)

$E \pm E_0$	$\log \varepsilon$	$\log(1\delta/D_{ox}T)$	$\log(1-e^{-UT})$	$\log e^{-\varphi}$	$-\log(1-\varepsilon Z)$	$\log(I/I_g-I)$
0.1	-2.000	-3.487	0	-1.691	0	-7.178
0.08	-1.658	-3.487	0	-1.353	0	-6.498
0.06	-1.377	-3.487	0	-1.015	0	-5.879
0.04	-1.032	-3.487	0	-0.642	0	-5.161
0.02	-0.728	-3.487	0	-0.338	0	-4.553
0.0	-0.438	-3.487	0	0	0	-3.925
-0.02	-0.234	-3.487	0	0.338	0	-3.383
-0.04	-0.120	-3.487	0	0.642	0.001	-2.964
-0.06	-0.056	-3.487	0	1.015	0.002	-2.526
-0.08	-0.026	-3.487	0	1.353	0.004	-2.156
-0.1	-0.014	-3.487	0	1.691	0.008	-1.802
-0.12	-0.007	-3.487	0	2.032	0.016	-1.446
-0.14	-0.0045	-3.487	0	2.362	0.034	-1.096
-0.16	-0.004	-3.487	-0.002	2.710	0.080	-0.703
-0.18	0	-3.487	-0.030	3.040	0.175	-0.302
-0.2	0	-3.487	-0.150	3.380	0.358	0.101
-0.22	0	-3.487	-0.357	3.720	0.614	0.490
-0.24	0	-3.487	-0.640	4.060	0.821	0.754
-0.26	0	-3.487	-0.944	4.500	1.244	1.313
-0.28	0	-3.487	-1.272	4.740	1.444	1.425
-0.3	0	-3.487	-1.607	5.100	1.523	1.529

In the case of quasi-reversible or irreversible neopolarograms, the functions ε and U from eq. (12) become

$$\varepsilon = k_s\, l^{-1}\, e^{(1-\alpha)\varphi}\, (L_1^2 - 4L_1 \Lambda_1)^{-1/2}\, (y_1^{-1}\, e^{y_1^2 t_1}\, \operatorname{erfc}(y_1 t_1^{1/2}) - y_2^{-1}\, e^{y_2^2 t_1} \cdot \operatorname{erfc}(y_2 t_1^{1/2}))$$

$$U = k_s\, l^{-1}\, e^{(1-\alpha)\varphi}\, (1 + k_s\, \delta\, D_{ox}^{-1}\, e^{-\alpha\varphi})^{-1}$$

The function Z does not change. All the symbols have been already defined.

When the k_s value decreases, the function $-\log(1-\varepsilon Z)$ shifts towards more positive potentials, while the function $\log(1-e^{-UT})$ shifts to more negative potentials. The split between these functions causes a shift of the middle

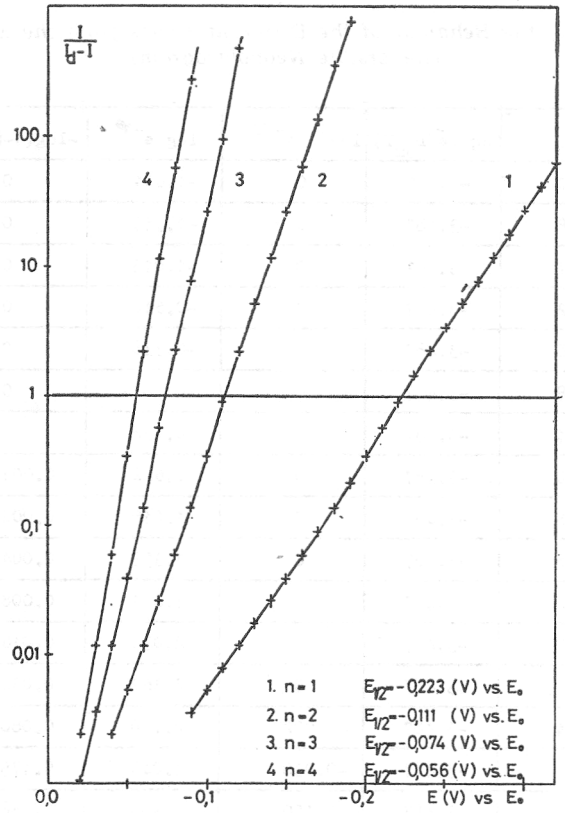

Figure 9. Logarithmic analysis of neopolarograms with various number of electrons transferred (theory).

part of the logarithmic analysis in the negative direction. In its lower part, the logarithmic analysis depends only on the terms $-\frac{nF}{RT}(E - E^0)$ and $\ln \frac{l\delta}{D_{ox}T}$ because the term $\ln \varepsilon$ has a very slight influence when quasi-reversible and irreversible neopolarograms are in question.

Finally, it must be emphasized that the deposition current (eq. (8)) is the exponential function of time. However, it should be noted that the exponential factor ($N/L=U$) is also the exponential function of the potential (see eq. (11) and eq. (13)). The function U tends to infinity when $E > E_o$, but to zero when $E < E^0$. This is the reason why the deposition current strongly depends on time at the potentials near E^0, but at more negative potentials it is independent of time. This effect was first noticed by Lee[12] with a rotating mercury electrode. It has also been described by Zirino and Kounaves[10] and Shuman and Cromer[11]. We, too, have obtained similar results with the digital simulation of neopolarograms. In our opinion, this fact is the main reason for a negative potential shift of the neopolarogram from the d. c. polarogram.

Figure 10. shows the results of the numerical analysis of eq. (12) under irreversible conditions. These results are in a good agreement with the digital simulation values for irreversible neopolarograms. It can be noticed that under these conditions the half-wave potential cannot be expressed explicitly.

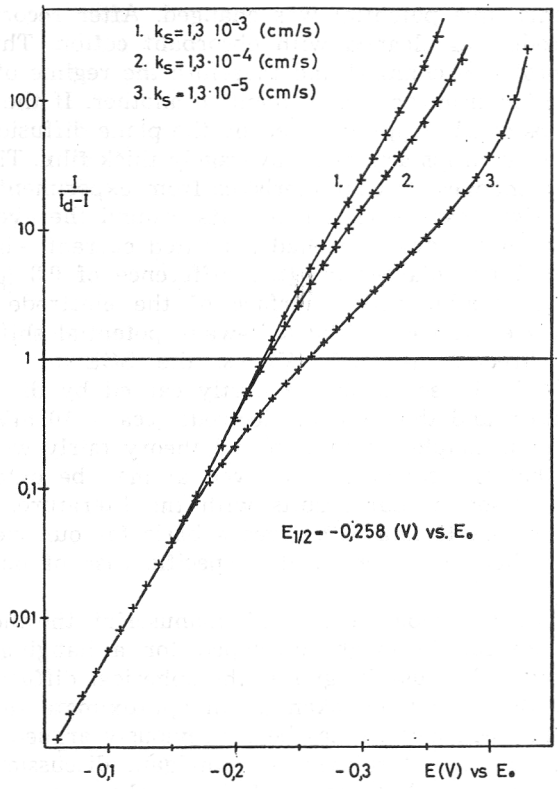

Figure 10. Logarithmic analysis of cathodic-current-integral neopolarograms for various values of the standard constant of the electrochem. reaction rate (theory).

DISCUSSION

If one wants to make a comparison between experimental and simulated results, a shift of the average values of half-wave potentials in a positive direction may be observed. Experimental data vary for about 30 (mV) and this may be attributed to a variation of the mercury layer thickness on an electrode. However, theoretical reconstructions of lead neopolarograms, with all experimental values of mercury layer thicknes, gave a variation of the half-wave potential values of about 20 (mV). The quantity of mercury electrolyzed on the electrode was calculated by an integration of cathodic current over the accumulation time. The cathodic current was measured from the shift of a recorder over the base line during the period of accumulation. There is serious doubt that a reduction of oxygen and hydrogen traces on an uncovered carbon surface can interfere with the mercury reduction. Thus, the calculated thickness of the mercury layer was too big, but no satisfactory method to check it has been found.

Theoretical calculations and simulations were performed assuming a uniform mercury layer over the whole surface of the carbon discs. According to Štulikova[13], this is only a very rough approximation, because mercury accumulated on the carbon surface in the form of drops in active places. The number and the volume of the drops depends on the accumulation potential. During experiments, this potential was changed. After recording neopolarograms, the electrode was cleaned with obsorbant cotton. Thus, the number of active places probably changed and therefore the regime of mercury accumulation changed too from one experiment to another. If the diffusion enveloping all the drops can be approximated by the plane diffusion, the electrode with small and bigger drops acts as an averagely thick film. This is the reason why the electrode changes its characteristics from experiment to experiment, which leads to a significant variation of data around the average value.

Simulated lead neopolarograms had a limited current which was similar to the experimental neopolarograms (the difference of 0.3 (μA) might have been caused by a smaller active surface of the electrode than the total graphite disk surface). However, the half-wave potential shifted by 15 (mV) in the positive direction (—0.512 (V) vs. the SCE in comparison with —0.527 (V) vs. SCE). These shifts are partly caused by diffusion potentials between the solution and the calomel electrode (cca. —10 mV). Nevertheless, we assume that, in principle, simulation and theory fairly well describe neopolarograms, so that the conclusions arrived at may be extended to a real system. The comparison of our results with the literature, especially with the work of Zirino and Kounaves[10], gives a basis for our views because we have proved that their data represent a specific case of our more general results.

In the course of the preparation of this manuscript, the theory of Shuman and Cromer[11] appeared. Although developed for a hanging mercury drop electrodes this theory, because it ignores the spherical diffusion towards and inside a mercury drop, may be taken as an approximate theory for planar thick mercury film electrodes, as has been previously argued[2] (approximative because of the inadequate treatment of amalgam discussion, for example, the way of calculating the bulk conc. of the amalgam and the introduction of a constant diffuse layer in the mercury drop). Nevertheless, being postulated on the same concepts (Nernst's diffusion layer concept) though the mathematical procedure was different, this theory and our mathematical model gave the same results. Indeed, except for some small differences which arose from our ignoring the amalgam diffusion through the mercury layer and a different mathematical approach, eq. (11) of this paper is equivalent to eq. (15) (for reversible) and eq. (21) for nonreversible charge transfers) of Shuman and Cromer's paper[11]. This is the best double-check for our mathematical model and a proof of our comments on Shuman and Cromer's theroy.

Finally, we may conclude that neopolarography is a well defined and carefully examined analytical technique offering a good possibility for the exploration of trace metal characteristics at very low concentration levels. The RGCDTMF electrode is very useful because of its high sensitivity ($\sim 10^{-9}$ dm^{-3}), easy maintenance and fairly good reproducibility of results. Rotating disk electrodes covered with constant thickness mercury film would give, perhaps, even better reproducibility than the permanently growing thickness mercury film electrodes described in this paper. However, their tranfer from

a vessel for the pre-electrolysis of the mercury to an experimental vessel might cause additional pollution of the experimental solution.

Acknowledgements. — The authors wish to express thanks to Dr. I. Ružić for help during the preparation of this work.

Acknowledgements are made to the Self Management Council for Scientific Research of S. R. Croatia for support of this work as well as to the National Bureau of Standards, Washington, D.C., U.S.A., for support of this work under Grant NBS/IG/-191/JF.

REFERENCES

1. M. Branica, D. M. Novak, and S. Bubić, *Croat. Chem. Acta* **49** (1977) 539.
2. M. Lovrić and M. Branica, *Croat. Chem. Acta* **53** (1980) 477.
3. S. Bubić and M. Branica, *Thalassia Jugoslav.* **9** (1973) 47.
4. M. Florence, *J. Electroanal. Chem.* **27** (1970) 273.
5. H. W. Nürnberg, P. Valenta, L. Mart, B. Raspor, and L. Sipos, *Freshius Z. Anal. Chem.* **282** (1976) 357.
6. L. Sipos, T. Magjer, and M. Branica, *Croat. Chem. Acta* **46** (1974) 1.
7. I. Šinko and J. Doležal, *J. Electroanal. Chem.* **25** (1970) 53.
8. V. Levič, *Physicochemical Hydrodynamics,* Prentice Hall, New York 1962.
9. D. K. Roe and J. E. A. Toni, *Anal. Chem.* **37** (1965) 1503.
10. A. Zirino and S. P. Kounaves, *Anal. Chem.* **49** (1977) 56.
11. M. S. Shuman and J. L. Cromer, *Anal. Chem.* **51** (1979) 1546.
12. T. S. Lee, *J. Amer. Chem. Soc.* **74** (1952) 5001.
13. M. Štulikova, *J. Electroanal. Chem.* **48** (1973) 33.

SAŽETAK

Simulirani i eksperimentalni neopolarogrami dobiveni s pomoću rotirajućih disk-elektroda

M. Lovrić i M. Branica

Analizirana su svojstva digitalno simuliranih reverzibilnih i nereverzibilnih neopolarograma. Uspoređeni su rezultati digitalne simulacije s eksperimentalnim neopolarogramima olova u perkloratnom mediju. Razvijena je teorija neopolarografije na tankoslojnim elektrodama.

CENTAR ZA ISTRAŽIVANJE MORA
INSTITUT »RUĐER BOŠKOVIĆ«
ZAGREB

Prispjelo 4 .veljače 1980.